Magnetic Modification of the External Surfaces in the MCM-41 Porous Silica: Synthesis, Characterization, and Functionalization

A. B. Bourlinos, A. Simopoulos, N. Boukos, and D. Petridis*

Institute of Materials Science, NCSR "Demokritos", Ag. Paraskevi Attikis, Athens 153 10, Greece

Received: January 24, 2001; In Final Form: May 21, 2001

Chemisorption of propionic acid vapors by an iron impregnated MCM-41 porous silica leads to the formation of iron−propionate species that upon pyrolysis can be transformed into γ-Fe_2O_3 nanoparticles of uniform size (~150 Å) and homogeneously dispersed on the external surfaces of the porous silica support. The effect of the carboxylic acid nature on the size of the magnetic particles was examined. The magnetically modified MCM-41 solid retains its crystallinity and large surface area and can be functionalized with various organosilicon ligands, e.g., $(CH_3O)_3SiCH_2CH_2CH_2NHCH_2CH_2NH_2$, to produce novel reconstructed MCM-41 derivatives without destroying the magnetic properties of the parent material. The various steps in the synthesis and functionalization, as well as the nature, size, and location of the particles into the final solids were studied by means of IR and XRD, bulk magnetic measurements, Mössbauer, BET, and TEM techniques.

Introduction

Mobil oil company, a few years ago, discovered a new family of silica-based mesoporous materials, designated as M41S.[1] A well-studied member of this family is the MCM-41 material, with an hexagonal arrangement of cylindrical pores between which an amorphous silicon dioxide network is interposed.[2,3] The large surface area possessed by MCM-41 materials (1000−1500 $m^2\ g^{-1}$), their tunable porosity[4,5] (with pore diameters ranging between 15 and 100 Å), and their uniform pore size distribution and thermal stability constitute some of the most attractive properties exhibited by these novel crystalline solids. A main drawback of these materials is their inactive chemical composition. Therefore, modification of the surface is necessary in order to endow the MCM-41 materials with desirable properties, such as catalytic, environmental, or even technological. Important modifications comprise the insertion of active metal centers into the silicon oxide network of the parent material for catalytic applications,[6,7] the grafting of organosilicon groups capable of binding metal ions or molecules for biological,[8] environmental,[9] and, in general, sensoring purposes, organically modified MCM-41 materials for triphase catalysis,[10] polymer-MCM-41 composites,[11] and, most interestingly, the formation of nanophase particles, for example, metal oxides of α-Fe_2O_3,[12,13] TiO_2,[14] and Rh_2O_3,[15] as well as metallic particles of Au[16] and Pt[17] supported onto the surface of the porous silica.

The literature reports little work on the synthesis of magnetically modified[18] MCM-41 materials with iron oxide particles. A simple synthesis of such magnetically modified MCM-41 material would undoubtedly be much welcome because of the simplicity of magnetic separation of porous silica in various catalytic, environmental, or other applications. Because of the well-defined and organized pores of an MCM-41 material, the latter is an excellent host matrix for the accommodation of various molecules, e.g., a conducting polymer thread, within its pore channels. In an envisioned application, the potential alignment of the MCM-41 particles in the direction of an applied magnetic field (due to its magnetic properties) would not only enable an intraparticle orientation of the accommodated species but also interparticle orientations, thus giving rise to novel and enhanced phenomena. In addition, magnetic iron oxides embedded in inorganic supports could find applications as fillers in the paint industry, in selective catalytic reactions, in wastewater environmental technology, in biotechnology, and in others.[19−21]

To fulfill this need, we report here the synthesis and characterization of γ-Fe_2O_3 nanoparticles embedded on MCM-41 porous silica. The synthesis relies on the wet impregnation method to first load porous silica with the $Fe(NO_3)_3{\cdot}9H_2O$ salt. The system is then subjected to a treatment with vapors of propionic acid, and finally, after calcination of the iron−propionate species, finely divided γ-Fe_2O_3 particles of uniform size embedded onto the external surfaces of the MCM-41 silica are obtained. The method has three advantages: is simple, soft, and of general use, since it has been already applied for the magnetic modification of other inorganic supports, including layered aluminosilicates and fumed silica.[22,23] The ability of the magnetic material for further modification is also presented.

Synthesis

Starting Materials. For the synthesis of the MCM-41 material, the following reagents were used: tetramethoxysilane (TMOS) and a 50% cetyltrimethylamonioum chloride aqueous solution (C16TMACl) from Merck-Schuchardt. For the wet impregnation method, the $Fe(NO_3)_3{\cdot}9H_2O$ salt was used (Merck). The following carboxylic acids were used for the vapor phase treatments: formic acid (85%, Carlo-Erba), glacial acetic acid (Riedel-deHaën), and propionic acid (99%, Merck). For the magnetic solid functionalization, the $(CH_3O)_3SiCH_2CH_2CH_2NHCH_2CH_2NH_2$ agent (Aldrich) was used.

Procedure. *(a) MCM-41*. The material was prepared according to a published route.[24] To a solution of 65.7 g of deionized water and 12.5 g of methanol, 3.6 g of a 50% aqueous solution of C16TMACl was added, followed by the addition of 9−12 drops of a 50% sodium hydroxide solution. A solution of 6.5 g of TMOS in 10 g of methanol was then added to the template solution. To the white precipitate, formed after a few seconds,

* To whom correspondence should be addressed.

10.1021/jp010286+ CCC: $20.00 © 2001 American Chemical Society
Published on Web 07/13/2001

10 mL of ethanol was added, and the mixture was stirred at room temperature for 3 h. The white solid was centrifuged and washed several times (7−8) with water and then spread on a glass plate for drying. The dried sample was finally calcined at 550 °C for 7 h under air at steps of 1 °C min^{-1}.

(b) Synthesis of the Magnetically Modified MCM-41 Material. In preparing the iron impregnated MCM-41 sample, we calculated the amount of added iron salt to give, after calcination, a product with 15% iron based on the formula $SiO_2 \cdot Fe_2O_3$. Specifically, 0.3 g of MCM-41 calcined at 550 °C was dispersed in 5 mL of methanol, and to the resulting mixture, 432 mg of $Fe(NO_3)_3 \cdot 9H_2O$ was added. After the mixture had been stirred for attaining a homogeneous dispersion (about 1 h), the solvent was rapidly removed at 80 °C. Without any washing, an almost white powder was received. The as-prepared iron impregnated sample was then exposed to vapors of propionic acid (0.5 mL) at 80 °C for 30−45 min in a closed vessel (volume: 300 cm^3). A pale reddish sample was obtained, which was finally calcined at 300 °C for 30 min in air in a small furnace. The final product exhibited macroscopic magnetic properties, as evidenced by its attraction to a permanent magnet. Iron determination in the final solid gave an iron content 1.5−2% lower than that theoretically expected.

(c) Surface Modification of the Magnetic Solid.[8] 0.34 g of the magnetically modified solid was suspended in 10 mL of toluene, and to the suspension, 1.5 mL of $(CH_3O)_3SiCH_2CH_2CH_2NHCH_2CH_2NH_2$ was added. The mixture was refluxed for 6 h under stirring, separated by centrifugion, washed well with toluene and acetone, and finally redispersed in acetone and dried by spreading over a glass plate.

Characterization. X-ray powder diffraction patterns were recorded on a Siemens D-500 diffractometer using CuK_a radiation. The IR spectra were taken in the form of KBr pellets with an FT-IR spectrometer of Bruker, Equinox 55/S model. Mössbauer spectra were recorded with a constant acceleration spectrometer with a 50mCi $^{57}Co(Rh)$ source moving at R. T., while the sample (absorber) was kept in a variable temperature cryostat. The parameters were obtained by a least-squares fitting program assuming Lorentzian line shapes. Isomer shift values are given with respect to metallic iron. Adsorption isotherms were taken on a nitrogen Autosorb 1 Quantacrome Corporation porosimeter at 77 K. The BET surface areas were calculated in the region 0.05−0.3 of relative pressures, while the mean pore diameters were calculated assuming a cylindrical pore model.[25] Magnetic measurements were carried out at room temperature with a Quantum Design magnetometer (SQUID). Finally, a CM20 Phillips instrument was used for the transmission electron microscopy study (TEM).

Results and Discussion

Synthesis. The parent MCM-41 sample was iron loaded by impregnation with an alcoholic ferric nitrate solution. This well-established method offers a uniform distribution of iron centers over the outer surfaces as much over the inner walls of the porous silica. The homogeneous dispersion of oligomeric iron ions over the MCM-41 surfaces is shown by the lack of detection of crystalline phase of $Fe(NO_3)_3 \cdot 9H_2O$ in the corresponding XRD pattern. As these iron centers are easily accessible to vapors of propionic acid, they can be converted to iron−propionate derivatives and finally upon calcination to nanophase magnetic particles. The ability of iron carboxylate compounds to be transformed upon pyrolysis into crystalline magnetic iron oxidic phases is known,[26,27] while the formation of iron−propionate precursor species in the present case is clearly established with IR spectroscopy from the presence of the 1590 cm^{-1} and 1448 cm^{-1} bands, due to the symmetric and asymmetric stretching vibrations of the $-COO^-$ bonds of the propionate anion in a binding mode of coordination.[28]

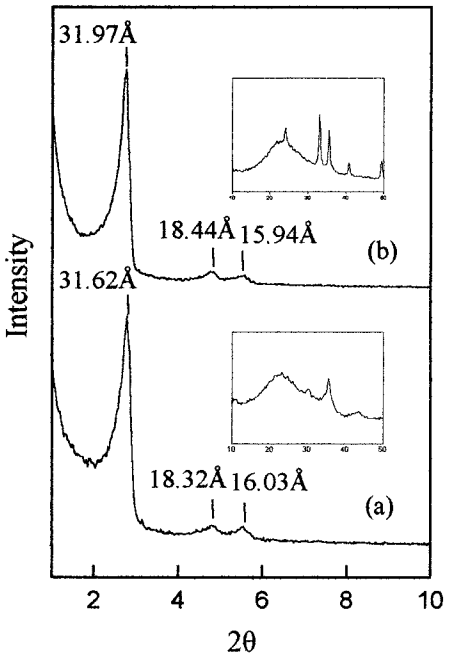

Figure 1. XRD patterns for an iron impregnated porous silica calcined at 300 °C after (a) and before (b) the propionic acid treatment.

Upon dispersing the magnetic solid in water, no coloration of the supernatant liquid or phase separation was observed. These observations, reflecting a strong adhesion of the iron oxide particles onto the silica surfaces, could be explained by the formation, during calcination, of Si−O−Fe bonds between the silica host matrix and the iron oxidic guest particles near their conducting surfaces.

At this point, it is important to clarify that for a certain iron loading (usually 5−20%) the magnetic modification of a solid in terms of its magnetic field strength requires the growth of large enough magnetic particles at the surfaces. This condition originates mainly from the dependence of the magnetic properties of a particle upon its volume.[29] For a given temperature, the smaller the particle size is, the smaller its magnetic strength will be and vice versa. Therefore, in the case of an MCM-41 material, magnetic modification can only arise from particles growing at the external surfaces of the solid and not from particles or clusters grown within the pores with diameters near 20 Å (vide infra). Bearing this in mind, we focus the main interest of this work on the presence of magnetic particles at the external surfaces of the silica and not inside its inner walls.

Characterization. Figure 1 shows the XRD patterns of a magnetically modified MCM-41 sample (a) and that of an iron impregnated sample calcined at 300 °C (b) without any propionic acid treatment. The inset patterns cover the 10−50° region which registers the presence of iron oxidic phases. We observe that the typical for an MCM-41 hexagonal array is maintained throughout the propionic acid and thermal treatments, while we also discern the appearance of a reflection near 36° marking the formation of γ-Fe_2O_3 nanophase particles with a mean diameter of 140 Å, as estimated from the Scherrer equation. Such particles, developed exclusively at the external surfaces of the MCM-41 silica, are responsible for the magnetic properties of the solid. Indeed, when an iron impregnated sample

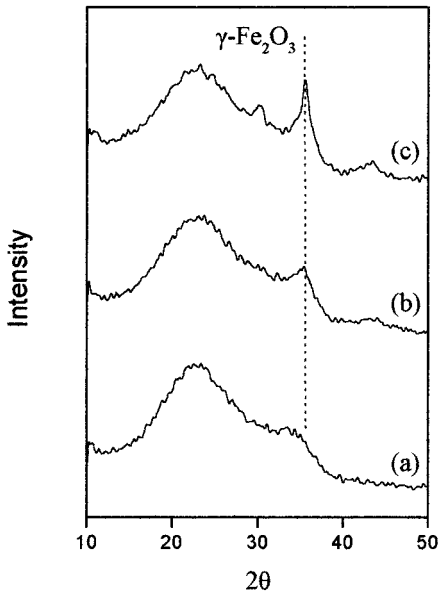

Figure 2. XRD pattern for an iron impregnated sample calcined at 300 °C after formic (a), acetic (b) and propionic acid (c) treatments.

was washed once with methanol to remove all or part of $Fe(NO_3)_3 \cdot 9H_2O$ from the external surfaces and subsequently exposed to propionic acid vapors and calcined, a non magnetic solid resulted (5wt % Fe) which did not show the characteristic reflection at ~36°. In the present case, it is possible that ultrafine γ-Fe_2O_3 particles may form in the inner walls of the porous silica. Mössbauer results, discussed latter, confirm this formation.

Essential condition for the magnetic phase formation is the carboxylic acid treatment. Thus, calcination of an iron impregnated solid before any propionic acid vapor treatment leads to a non magnetic product. The XRD pattern of this product exhibits characteristic reflections arising from the growth of large enough hematite particles (Figure 1b).

It is important to mention that when the carboxylic acid used in the vapor treatment was changed, magnetic particles of different sizes were obtained. The effect of the nature of carboxylic acid was examined by running the same sets of experiments but using formic or acetic acid instead of propionic. Both acids chelate the iron centers, as evidenced by IR spectroscopy, and do not affect the structural integrity of the MCM-41. The XRD results (Figure 2) indicate that the propionic acid treatment yields γ-Fe_2O_3 particles 140 Å in size, the acetic acid near 60 Å, while with formic acid the weak reflection at ~36° marks the formation of magnetic particles even smaller than 50 Å. A similar trend was also observed when we replaced the MCM-41 porous support with fumed silica, a nonporous solid, excluding in this way intra-pore effects to the size of the magnetic particles. These results indicate that there might be a connection between particle size and hydrophobic character of the carboxylic acid: the higher the hydrophobic character is, the larger the size will be. This is the case with propionic acid, which not only fulfills the chemical requirements for the magnetic phase formation (formic and acetic acid fulfill this requirement as well) but also tends to gather the highly dispersed iron centers and shape some iron−propionate aggregates of a critical size which can finally transformed into the magnetic phase after pyrolysis at 300 °C. It appears that the main driving force causing this self-concentration of iron centers onto the silica surfaces is the strong van der Waals interactions among the chelated iron species via the hydrocarbon groups. However, the butyric acid treatment gave similar results as the propionic acid.

TABLE 1: Hyperfine Parameters and Absorption Areas of the Spectral Components (P, Paramagnetic; M, Magnetic) of a Magnetically Modified MCM-41 Sample (A) and of a Similarly Obtained Solid But after Washing the Iron Sites from the External Surfaces (B)[a]

		M1			M2			P		
sample	T (K)	I. S.	H	A	I. S.	H	A	I. S.	QS	A
	4.2	0.48	529	50	0.46	488	50	–	–	–
A	78	0.45	520	55	–	–	–	0.46	0.88	45
	300	0.35	410	40	–	–	–	0.35	0.88	60
	4.2	0.48	490	100	–	–	–	–	–	–
B	78	–	–	–	–	–	–	0.46	0.90	100
	300	–	–	–	–	–	–	0.36	0.92	100

[a] I.S., isomer shift in mm/s; H, hyperfine field in KOe; QS: $e^2qQ/4$ in mm/s; A, relative absorption area (%)

The nature and size of the magnetic particles in the final solid (propionic and thermally treated) were unveiled by variable temperature Mössbauer spectroscopy. Figure 3 shows Mössbauer spectra at different temperatures of the magnetically modified MCM-41 sample (A) and of another sample prepared as the magnetic but subjecting the iron impregnated sample to a washing treatment in order to remove some $Fe(NO_3)_3 \cdot 9H_2O$ from its outer surfaces (B). Both samples display magnetic hyperfine structure at 4.2 K. Spectrum A was analyzed with two magnetic components and spectrum B with one component. The hyperfine parameters are listed in Table 1. In both cases, the quadrupole interaction is zero, indicating a cubic geometry around the iron site. Isomer shift and hyperfine fields values are typical of ferric iron and close to those of bulk γ-Fe_2O_3. As the temperature increases, a paramagnetic doublet appears to coexist with the magnetic component for case A, while for case B, the whole magnetic component transforms to a paramagnetic doublet at 78 K and above. This behavior is typical of superparamagnetism[30] and points to different particle sizes for the two samples—larger particles for the magnetic sample A and smaller for sample B that have undergone the washing treatment. In fact, by measuring various spectra in the temperature interval between 4.2 and 78 K (not shown), we have determined a blocking temperature (the temperature at which the spectral area of the magnetic and the paramagnetic components are equal) of 15 K for sample B. This blocking temperature corresponds to particles with sizes less than 15 Å.[31] Such particles presumably form within the pore channels of the MCM-41 silica. This hypothesis is further supported by the fact that the unwashed sample A has a magnetic component with larger hyperfine field (529kOe, Table 1) that is absent from the washed sample.

The magnetization versus applied field dependence of the magnetically modified MCM-41 sample at room temperature, shown in Figure 4, is characteristic of magnetic nanoparticles exhibiting reduced magnetization that is not saturated even at high applied fields owing to the superparamagnetic behavior of the crystallites. Extrapolation to the magnetization axis gives a saturation magnetization of $M_s = 3.2$ emu g^{-1}. The main contribution to this magnetic property derives from large particles lying at the external surfaces of the silica and not from those residing within its pores. In line with this assumption, the M_s value for the analogous solid obtained after removal of iron from the silica's outer surfaces was less than 0.5 emu g^{-1}.

Figure 5 presents the nitrogen adsorption−desorption isotherms of the magnetically modified sample (a) and that of the parent MCM-41 material (b). The similar shapes of the

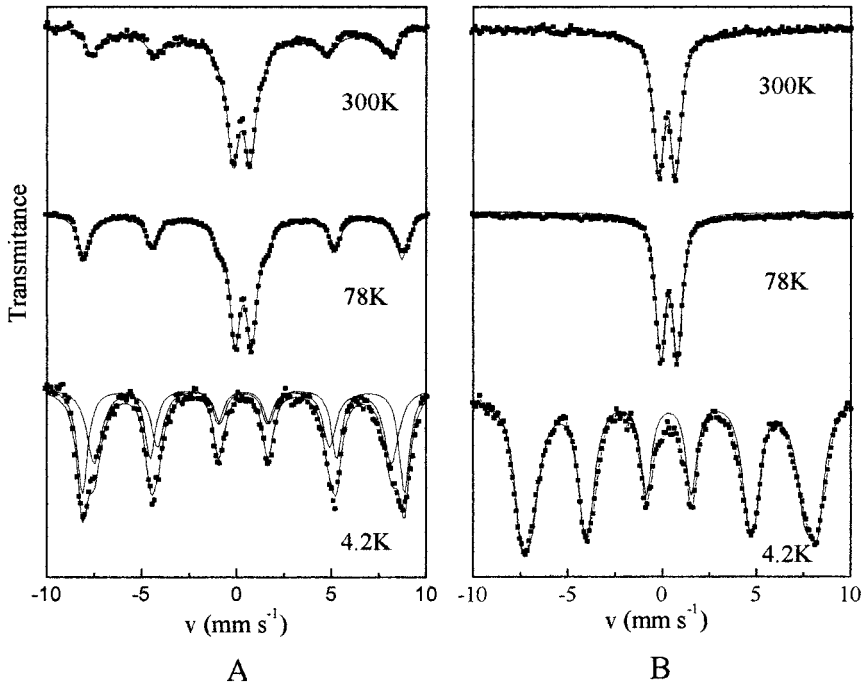

Figure 3. Variable temperature Mössbauer spectra of a magnetically modified MCM-41 solid (A) and of a similarly obtained solid but after washing the iron sites from the external surfaces (B).

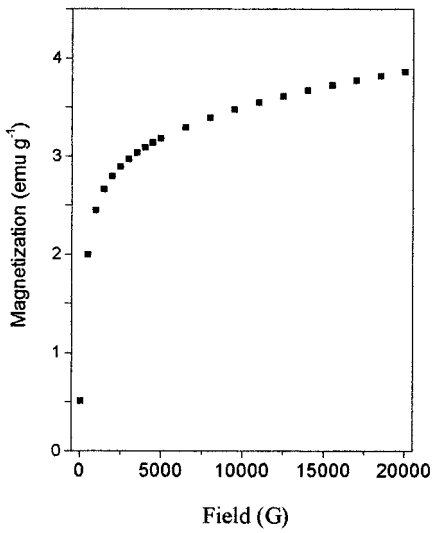

Figure 4. Magnetization vs applied field curve at room temperature for the magnetically modified sample.

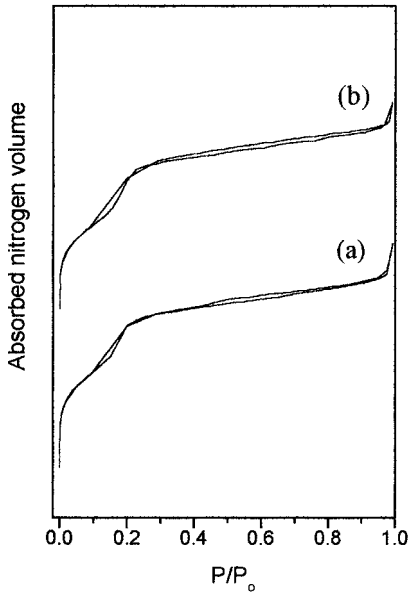

Figure 5. Adsorption−desorption isotherms for the magnetically modified (a) and non modified (b) MCM-41 samples.

isotherms is considered as a strong indication of a high dispersion of nanoparticles on the surfaces of the porous silica. Significant blocking of the pores entrance with particles would be expected to alter significantly the shape of the isotherm for the modified silica.[14] Both samples exhibit type IV isotherms with two narrow hysteresis loops that are characteristic of materials possessing cylindrical pores with pore dimensions less than 20 Å.[14] The magnetically modified sample as compared with the pure MCM-41 silica exhibits the following structural features: BET surface area, $S_{BET} = 1000$ versus 1200 $m^2\ g^{-1}$; pore radius, $r_p = 8$ versus 9 Å; pore volume, $V_p = 0.4$ versus 0.54 $cm^3\ g^{-1}$. Although somewhat reduced, the magnetically modified silica still retains the high surface area and large pore volume of the parent MCM-41 material. The observed changes may arise from the presence of ultrafine magnetic particles inside the pores of the silica.

Figure 6 shows two TEM micrographs for the magnetically modified sample. In the lower photograph, we observe the presence of agglomerated silica particles of irregular shape and with sizes between 0.1 and 0.5 μm, randomly decorated with well crystallized nano γ-Fe_2O_3 particles of uniform size averaged at 180 Å. The high-resolution TEM image of the sample (upper photograph) discloses that the silica particles retain the characteristic regular hexagonal pore arrangement of an MCM-41 material with a pore diameter close to that estimated from the BET analysis (∼20 vs 16−18 Å).

Functionalization. Once the magnetically modified porous silica retains most of the attractive properties of an MCM-41 material, with its high surface area and pore volume being the most important, the ability for further modification of its surfaces could be of particular value. Providing that the magnetic properties of the solid would not be eliminated by such modifications, the production of multifunctional materials in

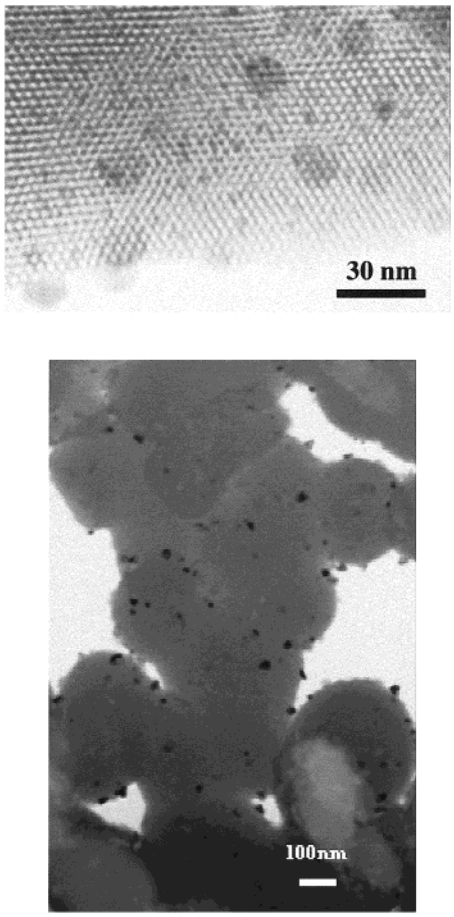

Figure 6. TEM micrographs for the magnetically modified MCM-41 material.

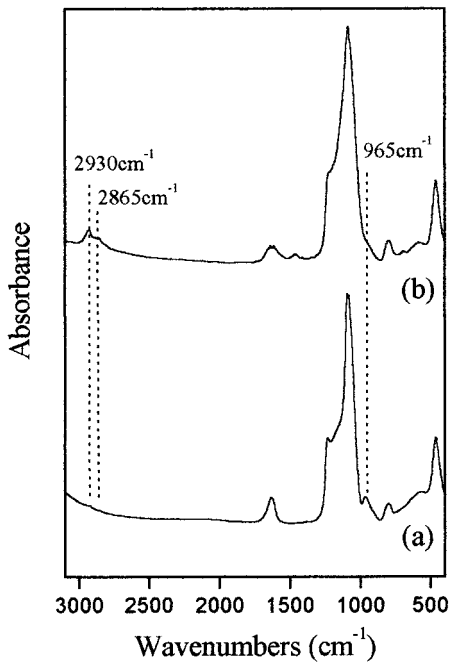

Figure 7. IR spectra of the magnetically modified MCM-41 porous silica before (a) and after (b) functionalization.

which the physicochemical properties of the particular modifier (polymer, dye, chelating agent) are combined with the properties of the magnetic particles is straightforward. For this purpose, we briefly present as an example the grafting of $(CH_3O)_3SiCH_2$-$CH_2CH_2NHCH_2CH_2NH_2$ (transition metal chelating agent, e.g. Cu^{2+}, Co^{2+}) onto the surfaces of the magnetically modified porous silica. The grafting is evidenced by IR spectroscopy. Figure 7 shows the IR spectra of the magnetically modified silica before (a) and after (b) its functionalization with the organosilicon ligand. Spectrum a is typical of a calcined silica, exhibiting absorption bands characteristic for a rigid silicon oxide network.[32] Most importantly, the material exhibits an absorption band at 965 cm^{-1} attributable to the presence of Si−OH bonds in the solid. Therefore, the magnetic solid, apart from its high surface area, exhibits and active sites for further modification. Indeed, after modification of the solid, the band at 965 cm^{-1} disappears, while new bands below 3000 cm^{-1}, attributable to the $-CH_2-$ moieties of the grafted ligand, are observed. These results clearly advocate grafting of the organosilicon ligand through condensation reactions with the free hydroxyl sites of the solid. The reconstructed in this way solid inherits the structural features of the parent MCM-41 silica together with its acquired magnetic properties ($M_s = 2.9$ emu g^{-1}).

Conclusions

The interaction of propionic acid vapors with an iron-impregnated MCM-41 porous silica leads to the formation of iron−carboxylate species that upon pyrolysis give rise to large enough γ-Fe_2O_3 nanoparticles (~150 Å) embedded onto the external surfaces of the porous silica and ultrafine particles (<15 Å) residing within the pores. For a certain iron loading, the magnetic particle size is primarily affected by the nature of the chelating carboxylic agent: the more hydrophobic the agent is, the larger the particle size will be, with propionic acid treatment affording the largest particles. As the final magnetic solid exhibits large surface area and free hydroxyl sites, it is accessible to further modification with an organosilicon compound with retention of its structural integrity and magnetic properties.

References and Notes

(1) Beck, J. S.; Vartuli, J. C.; Roth, W. J.; Leonowicz, M. E.; Kresge, C. T.; Schmitt, K. D.; Chu, C. T.-W.; Olson, D. H.; Sheppard, E. W.; McCullen, S. B.; Higgins, J. B.; Schlenker, J. L. *J. Am. Chem. Soc.* **1992**, *114*, 10834.

(2) Davis, M. E.; Chen, C.-Y.; Burkett, S. L.; Lobo, R. F. *Mater. Res. Soc. Proc.* **1994**, *346*, 831.

(3) Huo, Q.; Margolese, D. I.; Stucky, G. D. *Chem. Mater.* **1996**, *8*, 1147.

(4) Raman, N. K.; Anderson, M. T.; Brinker, C. J. *Chem. Mater.* **1996**, *8*, 1682.

(5) Tanev, P. T.; Pinnavaia, T. J. *Chem. Mater.* **1996**, *8*, 2068.

(6) Tanev, P. T.; Pinnavaia, T. J. In *Access in Nanoporous Materials*; Pinnavaia, T. J., Thorpe, M. F., Eds.; Plenum Press: New York, 1995; p 13.

(7) Corma, A. *Chem. Rev.* **1997**, *97* (6), 2373.

(8) Díaz, J. F.; Balkus, J. J.; Bedioui, F.; Kurshev, V.; Kevan, L. *Chem. Mater.* **1997**, *9*, 61.

(9) Mercier, L.; Pinnavaia, T. J. *Adv. Mater.* **1997**, *9*, 500.

(10) Howard; Harry, R. U.S. Patent 5,350,747, 1994.

(11) Frisch, H. L.; Mark, J. E. *Chem. Mater.* **1996**, *8*, 1735.

(12) Abe, T.; Tachibana, Y.; Uematsu, T.; Iwamoto, M. *J. Chem. Soc., Chem. Commun.* **1995**, 1617.

(13) Fröba, M.; Köhn, R.; Bouffaud, G. *Chem. Mater.* **1999**, *11*, 2858.

(14) Aronson, B. J.; Blanford, C. F.; Stein, A. *Chem. Mater.* **1997**, *9*, 2842.

(15) Mulukutla, R. S.; Asakura, K.; Kogure, T.; Namba, S.; Iwasawa, Y. *Phys. Chem. Chem. Phys.* **1999**, *1*, 2027.

(16) Okumura, M.; Tsubota, S.; Haruta, M. *Chem. Lett.* **1998**, *4*, 315.

(17) Junges, U.; Jacobs, W.; Martin, I. V.; Krutzsch, B.; Schüth, F. *J. Chem. Soc., Chem. Commun.* **1995**, 2283.

(18) MacLachlan, M. J.; Aroca, P.; Coombs, N.; Manners, I.; Ozin, G. A. *Adv. Mater.* **1998**, *10* (2), 144.

(19) Yang, B. L.; Hong, F.; Kung, H. H. *J. Phys. Chem.* **1984**, *88*, 2531.

(20) Navratil, J. D. In *Natural microporous Materials in Environmental Technology*; Misaelides, P., Macášek, F., Pinnavaia, T. J., Colleda, C., Eds.; NATO Science Ser. E.; Kluwer: Dordrecht, The Netherlands 1999; 362, 417.
(21) Penchev, I. P.; Hristov, J. Y. *Powder Technol.* **1990**, *61*, 103.
(22) Bourlinos, A. B.; Karakassides, M. A.; Simopoulos, A.; Petridis, D. *Chem. Mater.* **2000**, *12* (9), 2640.
(23) Bourlinos, A. B.; Simopoulos, A.; Petridis, D.; Okumura, H.; Hadjipanayis, G. *Adv. Mater.* **2001**, *13*, 289.
(24) Anderson, M. T.; Martin, J. E.; Odinek, J.; Newcomer, P. In *Access in Nanoporous Materials*; Pinnavaia, T. J., Thorpe, M. F., Eds.; Plenum Press: New York, 1995; p 29.
(25) Rierce, C. *J. Phys. Chem.* **1953**, *57*, 149.
(26) Jewur, S. S.; Kuriacose, J. C. *Thermochim. Acta*, **1977**, *19*, 195.
(27) Pinheiro, E. A.; Filho, P. P. A.; Galembeck, F. *Langmuir* **1987**, *3* (4), 445.
(28) Deacon, G. B.; Phillips, R. J. *Coord. Chem. Rev.* **1980**, *33*, 227.
(29) Martinez, B.; Balcells, L.; Roig, A.; Molins, E.; Obradors, X.; Rouanet, A.; Monty, C. In *Magnetic Hysteresis in Novel Magnetic Materials*; Hadjipanayis, G. C.; Ed.; NATO ASI Series, Series E; Applied Sciences; 1996; pp 338 and 351.
(30) Gangas, N. H.; Simopoulos, A.; Kostikas, A.; Yassoglou, N. J. *Clays Clay Mineral.* **1973**, *21*, 151.
(31) Vandenberghe, R. E.; De Grave, E. In *Mössbauer Spectroscopy Applied to Inorganic Chemistry*; Long, G. J., Grandjean, F., Eds.,; Plenum Press: 1982; 3, 59.
(32) Kamitsos, E. I.; Patsis, A. P.; Kordas, G. *Phys. Rev. B* **1993**, *48*, 12499.